5-16-2017

Rayleigh-LIDAR Observations of Mid-Latitude Mesospheric Densities

Brandon S. Hustead
Utah State University

Lucas R. Priskos
Utah State University

Jonathan L. Price
Utah State University

Joshua P. Herron
Utah State University

Rayleigh-LIDAR Observations of Mid-Latitude Mesospheric Densities

[1)] A. Brandon S. Hustead, Lucas R. Priskos, Jonathan L. Price,
Vincent B. Wickwar, Joshua P. Herron

[1]*Department of Physics and CASS, Undergraduate Research, PHYS 4900, Utah State University, Logan Utah, 84321, United States of America.*

This research is an analysis of absolute densities throughout the mesosphere (45 km to 90 km). Although much research has gone into the study of temperatures and their variations occurring in our atmosphere, little has been done to research the densities and their variations. Due to the remoteness of the middle atmosphere there is a high degree of difficulty in making observations in the mesosphere. There are currently three major types of ground-based instruments used to sense the mesosphere remotely. They are atmospheric radars, LIDARs and optical spectrometers. As far as measuring density in the mesosphere LIDAR is the most efficient. A Rayleigh-scatter LIDAR operated at the Atmospheric LIDAR Observatory (ALO; 41.7° N, 111.8° W), as part of CASS (Center for Atmosphere and Space Studies), on the campus of Utah State University (USU) has collected extensive data between 1993 and 2004. This LIDAR is used to measure relative densities (which can be used to derive temperatures) throughout the mesosphere. An analysis is made with the absolute densities from the atmosphere reanalysis model ERA-20C (the European Reanalysis 20th century model.) by using the model densities at 45 km to calibrate the LIDAR observations made at USU. Thereby, converting the relative densities measured by the USU LIDAR into measurements of absolute densities. These densities are used to examine the density structure of the mesosphere, how it varies with altitude and time, possible atmospheric anomalies, along with annual or semiannual atmospheric variations. Monthly averages are used to compare density variations related to altitude and season. By normalizing the relative densities from the Rayleigh LIDAR observations to the absolute densities from the reanalysis models, these differences can be observed and analyzed to better characterize the neutral atmosphere and learn how it varies during the year.

I. INTRODUCTION

We are interested in the middle atmosphere, 45 to 90 km. While there are many observations of temperatures in this region, there are very few observations of densities. Just as it is with temperature, density varies with both season and altitude. By determining absolute density instead of temperature, we can see some different atmospheric variability.

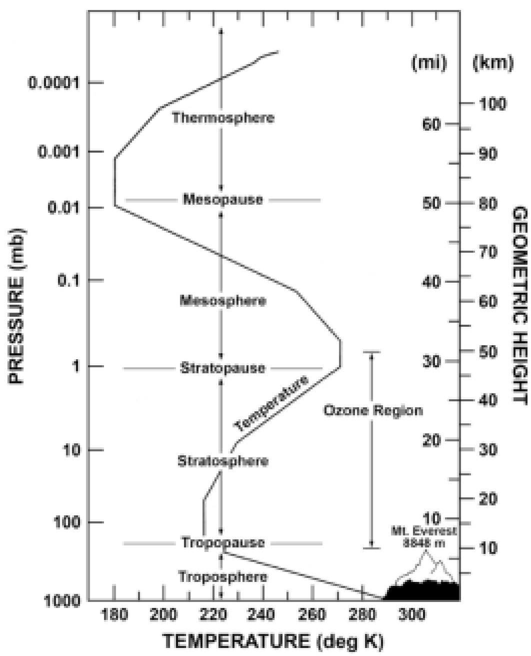

Figure 1. Vertical temperature structure of the atmosphere extending from the surface of the Earth to approximately 110-km altitude as given in the U.S. Standard Atmosphere, 1976. Two vertical coordinates are given: pressure on the left in millibars (1 mb = 1 hPa) and geometric altitude on the right (km). (Schlatter, 2009)

The middle atmosphere is where the Mesosphere resides. This particular region is difficult to measure because of its remoteness from both space and the ground. For altitudes up to about 30 km, measurements from methods such as balloon-borne data collection provide good measurements for model performance as they are not assimilated. The main problem is the lack of direct measurements above 30 km that are not normally part of the assimilation process in most models (Pichon et al., 2015). Differences found between different models could stem from temporal and spatial differences between instrument observations and model output, systematic problems that come with model physics, or even the different methods used for smoothing the model data. Models are also always improving. As computers get better, more detailed physics are included, and better methods for data collection are used, Model inputs are then modified to bring the model into agreement with the new data.

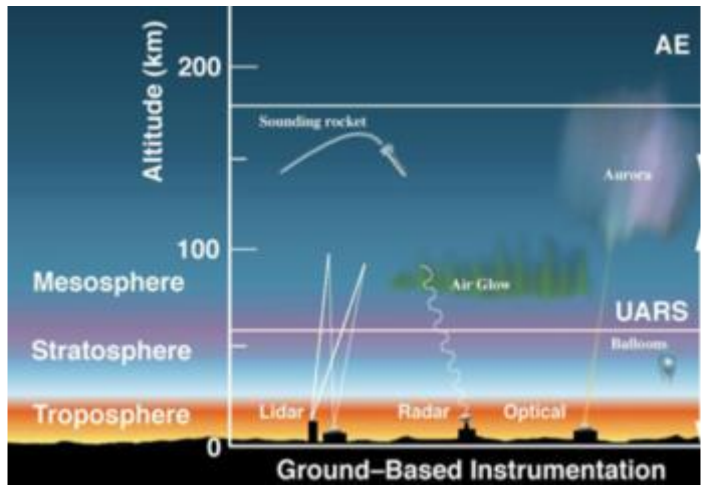

Figure 2. illustration of the various types of ground-based instrumentation and atmospheric phenomena that are used to collect atmospheric data as well as what altitudes they can cover. (NASA)

Different data collection methods include Sounding rockets, weather balloons, satellites, and observatories such as Lidar, Radar and Optical facilities.

Ground-based, Rayleigh-scatter lidars, such as the ALO-USU Rayleigh-scatter lidar, can provide access to the middle atmosphere. Their mesospheric observations can provide absolute temperatures and relative neutral number densities in the 35 km to 115 km or so altitude region.

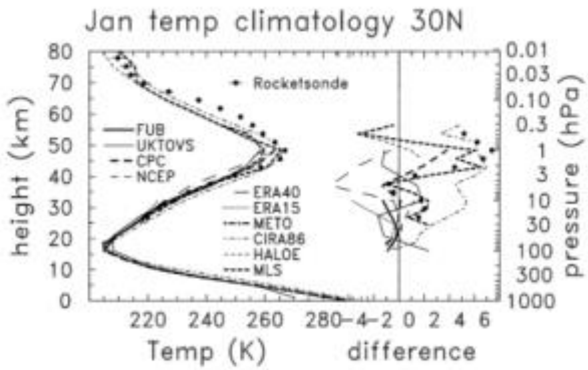

Figure 3. An example of data collected using rocketsonde temperature versus height measurements and a pressure obtained by a radiosonde to calculate density. This figure shows a comparison of Jan average rocketsonde temperature statistics at 30° N with similar data from various reanalysis models. (Randel et al., 2004)

II. METHODOLOGY

Rocketsonde observations are useful but can be expensive and infrequent. The Rayleigh lidar technique is the most effective method thus far.

Rayleigh lidar has been the major ground-based technique for making mesospheric observations of absolute temperatures. However, the Rayleigh lidar can also provide relative neutral number densities observations. Although these density observations have been much less studied because they are relative and not absolute. These relative number densities can still be used to calculate absolute densities by using a normalization of the relative density observations, and an outside source's measurement of absolute density at the same geometric height as the relative density's normalization.

This is done here by normalizing our relative neutral density LIDAR data to the calculations from our selected model, the European Reanalysis 20th century (ERA-20C) model. The ERA-20C model takes its calculations up to approximately 46 km.

A composite year is created using the LIDAR data by averaging 15 days before and after each day. These observations occurred over 11 years and is scaled to a constant at 45 km. An altitude of 45 km was chosen for comparing the LIDAR data to the reanalysis model because that is where the 2 data sets overlap.

A conversion however needs to be made to get density values from the ERA-20C data. In order to get density values at 45 km the models calculation of geopotential height is converted into geometric height using the equation

$$Z = \frac{g * z}{9.80} \qquad (1)$$

where Z is geometric height in meters, z is geopotential height, and g is the acceleration of gravity at the height of interest. The conversion from geopotential to geometric height takes into consideration the variation of gravitational acceleration with altitude. This conversion is done to put the reanalysis model values and the LIDAR data on the same altitude scale.

It is then necessary to convert the temperature and pressure levels in the reanalysis models into number densities. With those values, the number density can be obtained using the following form of the ideal gas law:

$$\rho = \frac{P}{T * k_b} \qquad (2)$$

where ρ is the number density, P is the pressure, T is the temperature associated with the pressure level, and k is Boltzmann's constant.

Because the ERA-20C model does not give us the density value at all heights, and because we are interested in getting an absolute density measurement at the geometric height of 45 km, after converting the reanalysis model's data into number densities for the best fit we ran a quadratic regression through the log of the densities at their given altitudes. Doing this allowed us to make an estimated calculation of the reanalysis models value for absolute density at 45 km.

Using this estimated calculation as the true density at 45 km, the relative densities from the LIDAR data can be converted to absolute densities by normalizing them to the reanalysis model's density values at 45 km for each of the corresponding days in the composite year.

III. BACKGROUND

The USU Atmospheric Lidar Observatory (ALO) is a green (532 nm) laser beam that is directed vertically into the atmosphere firing pulses of light at 30 Hz. Light from this laser beam reflected back is collected via 4 large mirrors, each with a diameter of 1.25 meters. The collected light is then sent through an optical fiber system connected to a chopper which is timed with the laser pulses via an Arduino microprocessor. The chopper is rotating at about 105 Hz with two openings. With the laser firing at 30 Hz we get a signal in about every 7^{th} opening. This causes only light to be received in from backscatter ranging between 38 km altitude and where no more signal is received (~325 km). After being put through the chopper, the light is then processed through a high-transmittance interference filter that only allows 532 nm light through. Thus, eliminating noise from outside light sources such as the moon, stars, and city lights. The light's signal is then amplified via a green-sensitive photomultiplier tube, converting the photons into photoelectrons via the photoelectric effect, and amplifying them by 10^7. Lastly the photoelectrons are measured by a digital counter every 250 ns, corresponding to an altitude resolution of 37.5 m. More photons are scattered back when the density is higher and vice versa. The ratio of major mesospheric neutral constituents, N_2 and O_2, is assumed constant, giving rise to a constant Rayleigh backscatter coefficient in the mesosphere. Above 45 km, the atmospheric transmission is taken to be 1.00.

IV. PROCEDURE

After removing the days from the ERA data that we didn't have data for in the LIDAR observations, and removed LIDAR data that was flagged bad for having measurements outside the norm, we made a composite year of relevant data. After eliminating the bad nights, we were left with 713 nights of observations covering 320 nights out of the 365 nights in a regular year. The majority of the 320 nights were accounted for by an accumulation of several nights of observations on that same particular day. Most of the nights that we were missing came out of the December and January months. This could be due to a number of reasons. It could be because of bad weather, students getting ready for finals and the end of the year holidays keeping the LIDAR observatory from running. The resultant being a noticeable discontinuity between the December to January months. Overall the relevant data still gives us a good picture of what is happening to the atmospheric density above 45 km.

After converting the reanalysis model's data into number densities, we were then able to take the LIDAR's relative density values above 45 km and the ERA model density value at 45 km to calculate the absolute number density values for altitudes at and above 45 km. Error for those values were then calculated by using a RMS value from the profiles in each of the 31-day by 11-year averages. This error represents a combination of measurement uncertainty and geophysical variability. After gathering the relevant data, we analyzed certain points of interest. We looked into the relationship between densities below and above 65 km. 65 km being the crossover point in temperature where rising above 65 km you reach the coldest part of the atmosphere in summer. We looked into how the density varies in magnitude as you rise in altitude. Lastly looking into any seasonal changes, we could observe from the resultant data.

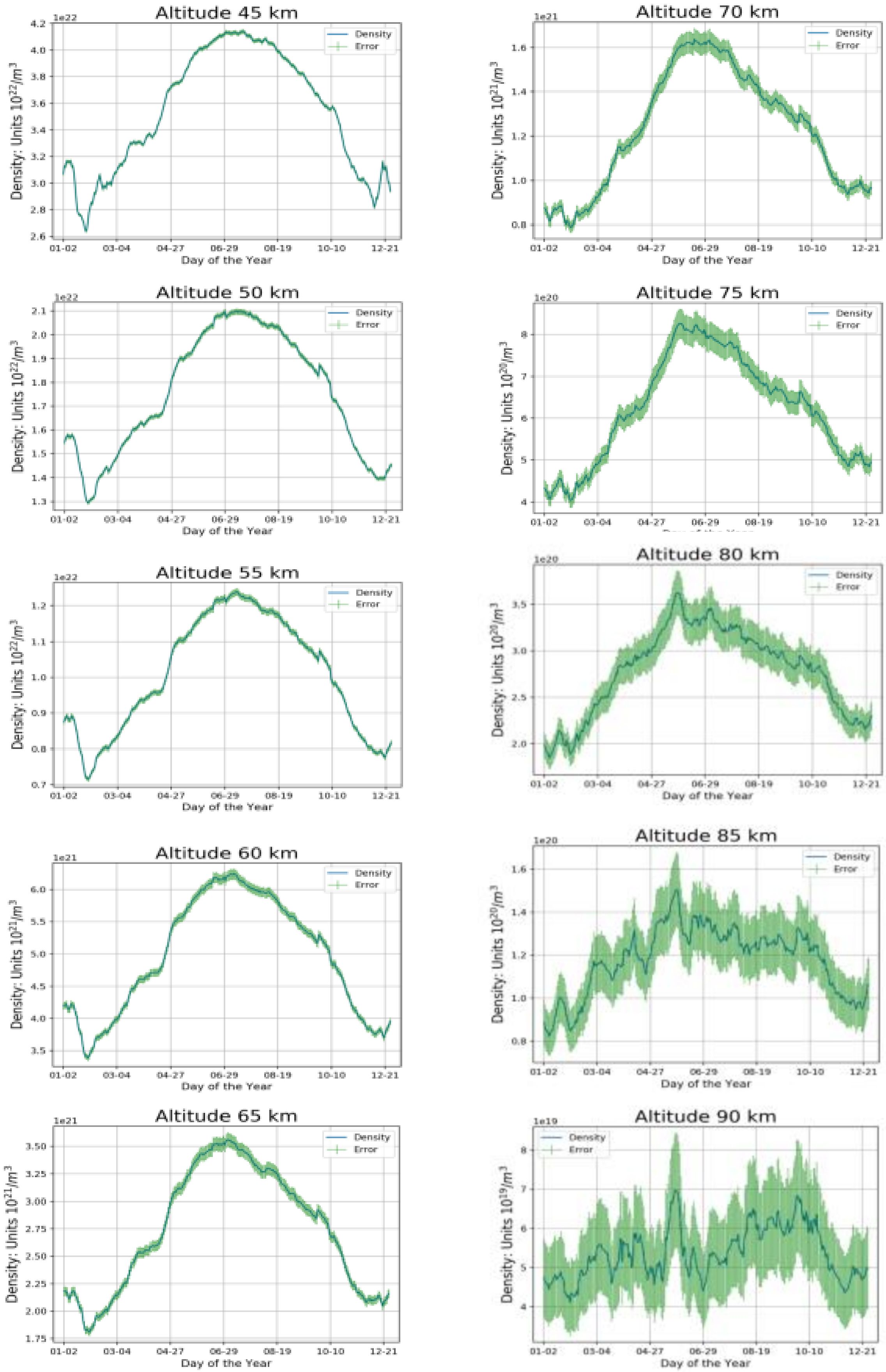

Figure 4. Number density values and Error Bars normalized to the ERA-20C reanalysis model over a composite year with altitudes between 45 and 90 km taken at 5 km intervals. The error bars are based on the standard deviation of the mean.

V. Analysis

Comparing above and below 65 km in figure 4, you can see some noticeable differences. One noticeable difference is that the relative max density during the time frame between January and February isn't as distinct above 65 km as it is below. This shows that whatever might be causing this peak in density isn't as prevalent above 70 km. This could be some form of cooling below 65 km or some sort of heating above 65 km during the month of January. Most likely this effect has to do with the transitioning period from winter into spring. Summer relative density maximums occur centered on late June at 70 km, at 85 km in mid May, shows up at 60 km in early July, and remains in early July below 60 km. This is fairly noticeable and shows summer as the densest time period of the mesosphere.

There is a relative maximum density right at the end of September that is quite noticeable for all altitudes. This occurs right before reaching a dramatic drop of density at the beginning of October. There is also a slight dip at each altitude after the summer max peak is reached. This dip appears to get more dramatic at higher altitudes. These two phenomena could be the transitioning from summer to fall, and from fall to winter.

The uncertainties at 90 km are noticeably large because the received signal is weaker and fewer nights go into making up the resulting average at that altitude. Because of the large uncertainties, it becomes unclear as to what the figure is showing.

While observing these densities one must keep in mind the magnitude of the densities we are observing. The number density of 10^{22} particles per cubic meter at 45 km is enough to be considered a rough vacuum by engineers and chemists (Weissier, 1990). In relation to Loschmidt's constant which is the standard number density under standard conditions (0º C and pressure of 1 Atmosphere) measuring at 2.6868×10^{25} particles per cubic meter. At 45 km you can see that we are already three orders of magnitude less than under standard conditions at the earth's surface. At 65 km you are one more order of magnitude less and at that rate by 90 km we are at a number density 6 magnitudes less than the standard number density given by Loschmidt's constant. That means it is about 1 million times less dense at 90 km than it is at the earth's surface.

Although pressure itself usually has no physical significance in vacuum systems, it is traditional to use this parameter as a measure of the degree of vacuum. The customary unit is presently the torr although one expects the SI unit of pressure (the Pascal) to become more common in the near future (Zussupov, 2014). At 1 mb (~45 km) it is considered a medium vacuum until you reach 0.001 mb (~90 km) at which it is then considered a high vacuum. To put this into perspective, upon reaching an altitude such as 80.5 km you have reached the U.S. definition of space flight.

VI. CONCLUSION

Throughout the middle atmosphere (from 45 to 90 km) at a mid-latitude site, we have determined the number density profiles of the middle atmosphere region by normalizing the relative densities from Rayleigh LIDAR observations to the densities from the ERA-20C reanalysis model. It is clear that future research is needed to better understand this region, and that advancements in technology have helped us reach this hard-to-reach area of our atmosphere. We were able to make observations on how the density profile changes due to altitude and time. we can see these changes evident through the time periods where there is a change in season occurring.

VII. FUTURE WORK

Future work can be done to compare other models using the same method. Reanalysis models such as the Japanese 55-year Reanalysis (JRA-55), National Centers for Environmental Prediction model (NCEP), and NASA's Modern-Era Retrospective analysis for Research and Application, Version 2 (MERRA-2) can also be used to obtain densities and examine trends in mesospheric density variations. The recent LIDAR upgrade and future planned upgrades would also allow an examination of density variations over a wider span of altitude. At higher altitudes, these densities and temperatures would provide a bottom boundary condition for thermospheric models, which are, for instance, used for orbital and reentry predictions.

ACKNOWLEDGMENTS

We gratefully acknowledge support from Utah State University, the USU College of Science and Physics Department, and Personal Contributions. The data acquisition was supported by grants from the Atmospheric Sciences Division of NSF. We acknowledge David Barton for his previous work on the data analysis. We acknowledge the ERA-20C reanalysis team for the use of their model.

REFERENCES

"APL Civil Space: Science." *APL Civil Space: Science*, NASA, civspace.jhuapl.edu/Science/index.php. Accessed Mar. 2017.

Dee, D. P., Uppala, S. M., Simmons, A. J., Berrisford, P., Poli, P., Kobayashi, S., Andrae, U., Balmaseda, M. A., Balsamo, G., Bauer, P., Bechtold, P., Beljaars, A. C. M., van de Berg, L., Bidlot, J., Bormann, N., Delsol, C., Dragani, R., Fuentes, M., Geer, A. J., Haimberger, L., Healy, S. B., Hersbach, H., Hólm, E. V., Isaksen, L., Kållberg, P., Köhler, M., Matricardi, M., McNally, A. P., Monge-Sanz, B. M., Morcrette, J.-J., Park, B.-K., Peubey, C., de Rosnay, P., Tavolato, C., Thépaut, J.-N. and Vitart, F. (2011), The ERA-Interim reanalysis: configuration and performance of the data assimilation system. Q.J.R. *Meteorol. Soc*., 137: 553–597. doi: 10.1002/qj.828

"Determination of Altitude by Measurement of Air Pressure and Temperature*." Journal of the Franklin Institute*, vol. 238, no. 6, 1944, pp. 453–454., doi:10.1016/s0016-0032(44)91082-3.

Hocke, K. "Inversion of GPS Meteorology Data." *Annales Geophysicae*, vol. 15, no. 4, 1997, p. 443., doi:10.1007/s005850050458.

Jens1973. "Pressure Altitude Derived." *Scribd*, Scribd, de.scribd.com/document/62271713/Pressure-Altitude-Derived. Accessed 4 May 2017.

Miers, Bruce T., et al. "Short Time Period Atmospheric Density Variations and Determination of Density Errors From Selected Rocketsonde Sensors." *Monthly Weather Review*, vol. 100, no. 3, 1972, pp. 189–195., doi:10.1175/1520-0493(1972)100<0189:stpadv>2.3.co;2.

Morris, Ray, and Damian Murphy. "The Polar Mesosphere." *Physics Education*, vol. 43, no. 4, 2008, pp. 366–374., doi:10.1088/0031-9120/43/4/003.

1967. NASA Technical Report 316

"ORBITEC." *ORBITEC*, www.orbitec.com/documents/Orbitec_Vacuum_Reference.pdf.

Pichon, A. Le, et al. "Comparison of Co-Located Independent Ground-Based Middle Atmospheric Wind and Temperature Measurements with Numerical Weather Prediction Models." *Journal of Geophysical Research*: Atmospheres, vol. 120, no. 16, 2015, pp. 8318–8331., doi:10.1002/2015jd023273.

Randel, William, Petra Udelhofen, Eric Fleming, Marvin Geller, Mel Gelman, Kevin Hamilton, David Karoly, Dave Ortland, Steve Pawson, Richard Swinbank, Fei Wu, Mark Baldwin, Marie-Lise Chanin, Philippe Keckhut, Karin Labitzke, Ellis Remsberg, Adrian Simmons, and Dong Wu. "The SPARC Intercomparison of Middle-Atmosphere Climatologies." *Journal of Climate* 17.5 (2004): 986-1003.

Schlatter, Thomas W. "Atmospheric Composition and Vertical Structure." *Environmental Impact and Manufacturing*, vol. 6, 2009.

Weissler, G. L. Vacuum *Physics and Technology*. San Diego, Acad. Press, 1990.

Zhussupov, Murat. "Features of Loschmidt's Number and Its Theoretical Frontiers." *International Journal of Fundamental Physical Sciences*, Sept. 2014, pp. 62–71., doi:10.14331/ijfps.2014.330067.